

# A Green and Facile Approach for Synthesis of Magnetite Nanoparticles

Akl M. Awwad<sup>1,\*</sup>, Nidá M. Salem<sup>2</sup>

<sup>1</sup>Royal Scientific Society, El Hassan Science City, Amman, Jordan

<sup>2</sup>Department of Plant Protection, Faculty of Agriculture, Jordan University, Amman, Jordan

**Abstract** This paper presents a facile, rapid and green method to prepare magnetite (Fe<sub>3</sub>O<sub>4</sub>) nanoparticles in one step reaction. In this method, an aqueous solution of ferric chloride hexa hydrate, ferrous chloride tetra hydrate (2/1 molar ratio) was mixed with carob leaf extract and heated for 5 minutes at 80 °C. The magnetite nanoparticles were characterized by scanning electron microscopy (SEM), thermogravimetric analysis (TGA), Fourier transform infrared spectroscopy (FT-IR) and X-ray diffraction (XRD). XRD analysis showed that the magnetite nanoparticles are well-monodisperse with 8 nm of average diameter. A possible synthesis mechanism of magnetite nanoparticles was presented at the same time.

**Keywords** Green Synthesis, Carob Leaf Extract, Magnetite Nanoparticles, Characterization

## 1. Introduction

Recently, an extensive research has been focused on nano-structured magnetite because it possesses unique magnetic and electric properties and its application in medical diagnosis and therapy, target drug delivery, magnetic resonance imaging, cancer hyperthermia treatment and nano-sorbents in environmental engineering[1-10]. Various methods of synthesizing magnetite nanoparticles have been developed such as Chemical precipitation method, which involves co-precipitation of ferric ions Fe(III) and ferrous ions Fe(II) by sodium hydroxide NaOH or ammonia solution NH<sub>3</sub>·H<sub>2</sub>O[11-13], thermal decomposition of organic iron precursor in organic solvents[14-16], Polyol process[17], sol-gel method[18], sonochemical synthesis[19,20], surfactants[21], solvothermal synthesis[22] hydrothermal synthesis [23,24], mechano-chemical processing[25] and emulsions technique[26,27]. In this study, we propose a rapid, non-toxic, facile and green synthesis route to prepare magnetite nanoparticles in only one step reaction. Ferric chloride hexa hydrate and ferrous chloride tetra hydrate, carob leaf extract and sodium hydroxide were used as starting materials. Magnetite nanoparticles can be obtained in a relatively low temperature range 80-85 °C. The synthesized magnetite nanoparticles were characterized by X-ray diffraction (XRD), scanning electron microscopy (SEM) and Fourier transform infrared (FT-IR).

## 2. Materials and Methods

### 2.1. Materials

Ferric chloride hexa hydrate (FeCl<sub>3</sub>·6H<sub>2</sub>O, AR), ferrous chloride tetra-hydrate (FeCl<sub>2</sub>·4H<sub>2</sub>O, AR) and sodium hydroxide (NaOH) were purchased from Aldrich Chemicals. Sterile distilled water obtained from our biotechnology laboratory with conductivity 1 μS/cm.



**Figure 1.** A picture of carob leaves and aqueous carob leaf extract

\* Corresponding author:

akl.awwad@yahoo.com (Akl M. Awwad)

Published online at <http://journal.sapub.org/nn>

Copyright © 2012 Scientific & Academic Publishing. All Rights Reserved

## 2.2. Preparation of Carob Leaf Extract

Carob leaves, Figure 1 were collected from carob trees at campus of Royal Scientific Society, Amman, Jordan. The leaves were washed several times with distilled water to remove the dust particles and then sun dried to remove the residual moisture. The dried carob leaves were cut to small pieces and boiled in 250 ml glass beaker along with 200 ml of sterile distilled for 5 minutes. After boiling, the colour of the aqueous solution changed from watery to yellow colour and allowed to cool to room temperature. The aqueous extract of carob leaf was separated by filtration with Whatman No.1 filter paper and then centrifuged at 1200 rpm for 5 minutes to remove heavy biomaterials. The carob leaf extract was stored at room temperature to be used for green synthesis of magnetite. Figure 1 shows a picture of carob leaves and carob leaf extract (yellow colour).extracted by sterile distilled water with boiling at a constant temperature, 80°C for 5 minutes.

## 2.3. Synthesis of Magnetite Nanoparticles

In this study, magnetite nanoparticles ( $\text{Fe}_3\text{O}_4$ ) synthesized as follows: 0.53 g of  $\text{FeCl}_2 \cdot 4\text{H}_2\text{O}$  and 1.11 g of  $\text{FeCl}_3 \cdot 6\text{H}_2\text{O}$  (1/2 molar ratio) were dissolved in 100 mL of sterile deionized water in a 250 mL beaker and heated at 80°C under mild stirring using magnetic stirrer and under atmospheric pressure. After 10 minutes, 5 mL of the aqueous solution of carob leaf extract was added to the mixture, immediately the yellowish colour of the mixture changed to reddish brown colour. After 5 minutes, 20 mL of sodium hydroxide aqueous solution was added to the mixture with rate 3 mL/min for allowing the magnetite precipitations uniformly. From the first addition of sodium hydroxide the reddish brown mixture changed to black suspended particles. The mixture was allowed to cool down to room temperature. and the magnetite nanoparticles were obtained by decantation, dilution with sterile distilled water and centrifugation to remove heavy biomaterials of carob leaf extract. The magnetite nanoparticles were purified by dispersing in sterile distilled water and centrifugation three times. The magnetite particles are divided into two parts. In the first part, the  $\text{Fe}_3\text{O}_4$  nanoparticles are remained in the sterile distilled water without any additives as prepared. The stability of magnetite suspended nanoparticles in sterile distilled water for more than two weeks. In the second part, the magnetite nanoparticles after purification were dried overnight at 80°C for XRD, TGA, SEM and FTIR analysis.

## 2.4. Characterization

Magnetite ( $\text{Fe}_3\text{O}_4$ ) nanoparticles synthesised by this green method were examined by X-ray diffractometer (Shimadzu, XRD-6000) equipped with  $\text{CuK}\alpha$  radiation source using Ni as filter at a setting of 30 kV/30mA. All XRD data were collected under the experimental conditions in the angular range  $3^\circ \leq 2\theta \leq 50^\circ$ . FT-IR spectra of carob leaf extract and magnetite nanoparticles was obtained in the range 4000-400  $\text{cm}^{-1}$  with FT-IR spectrophotometer (IR-Prestige 21,

Shimadzu) using KBr pellet method. Thermogravimetric analysis (TGA) was performed under nitrogen atmosphere at a heating rate of 10°C/min from room temperature up to 700°C using NetzschSta 449 C analyzer. Scanning electron microscopy (SEM) analysis of synthesized magnetite nanoparticles was done by SEM machine, Hitachi S-4500. Thin films of magnetite nanoparticles were prepared on a carbon coated copper grid by just dropping a very small amount of the sample on the grid, extra solution was removed using blotting paper and then the film on the SEM grid were allowed to dry by putting it under a mercury lamp for 5 minutes. UV-vis spectroscopic studies were carried out using Shimadzu UV-1601 spectrophotometer.

## 3. Results and Discussion

XRD is an effective characterization to confirm the crystal structure of the synthesized magnetite nanoparticles. The XRD spectrum of magnetite nanoparticles is presented in Figure 2. The  $2\theta$  peaks at 18.55°, 30.81°, 36.48°, 43.52°, 54.59°, 56.83° and 62.34° are attributed to the crystal planes of magnetite at 111, 220, 311, 222, 400, 422 and 511, respectively. The magnetite nanoparticles are well-crystalline and the position and the relative intensity of the diffraction peaks match well with the standard XRD data for bulk magnetite (JCPDS file No. 19-0629). The average particle sizes of the synthesized magnetite nanoparticles were calculated using Debye-Scherrer formula [13,28]:

$$D = K \lambda / \beta \cos \theta \quad (1)$$

where

D = the mean diameter of nanoparticles

$\beta$  = the full width at half-maximum value of XRD diffraction lines.

$\lambda$  = the wavelength of X-ray radiation source 0.15405 nm.

$\theta$  = the half diffraction angle –Bragg angle

K = the Scherrer constant with value from 0.9 to 1.

The particle sizes is determined by taking the average of the sizes at the peaks was found 8 nm.

The FT-IR spectra of carob leaf extract is given in Figure 3. A broad band between 3174 and 3442  $\text{cm}^{-1}$  centered at 3325  $\text{cm}^{-1}$  are due to the N-H stretching and bending vibration of amine group  $\text{NH}_2$  and O-H the overlapping of the stretching vibration of attributed for water and carob leaf extract molecules. The peak at 2931  $\text{cm}^{-1}$  could be assigned to the stretching vibrations of  $-\text{CH}_3$  and  $\text{CH}_2$  functional groups. The shoulder peak at 1712  $\text{cm}^{-1}$  is assigned for C=O stretching mode indicating the presence of  $-\text{COOH}$  group in the carob leaf extract. The strong band at 1604  $\text{cm}^{-1}$  and the shoulder peak at 1465  $\text{cm}^{-1}$  are identified as the amide I and amide II, which arise due to C=O and NH stretching vibrations in the amide linkage of the protein. The peaks at 1311 and 1222  $\text{cm}^{-1}$  can be assigned to the C-O group of polyols. The peak at 1076  $\text{cm}^{-1}$  corresponds to C-N stretching vibrations of aliphatic amines. FT-IR spectroscopy confirmed that the carob leaf extract has the ability to act as reducing agent and stabilizer for magnetite nanoparticles.

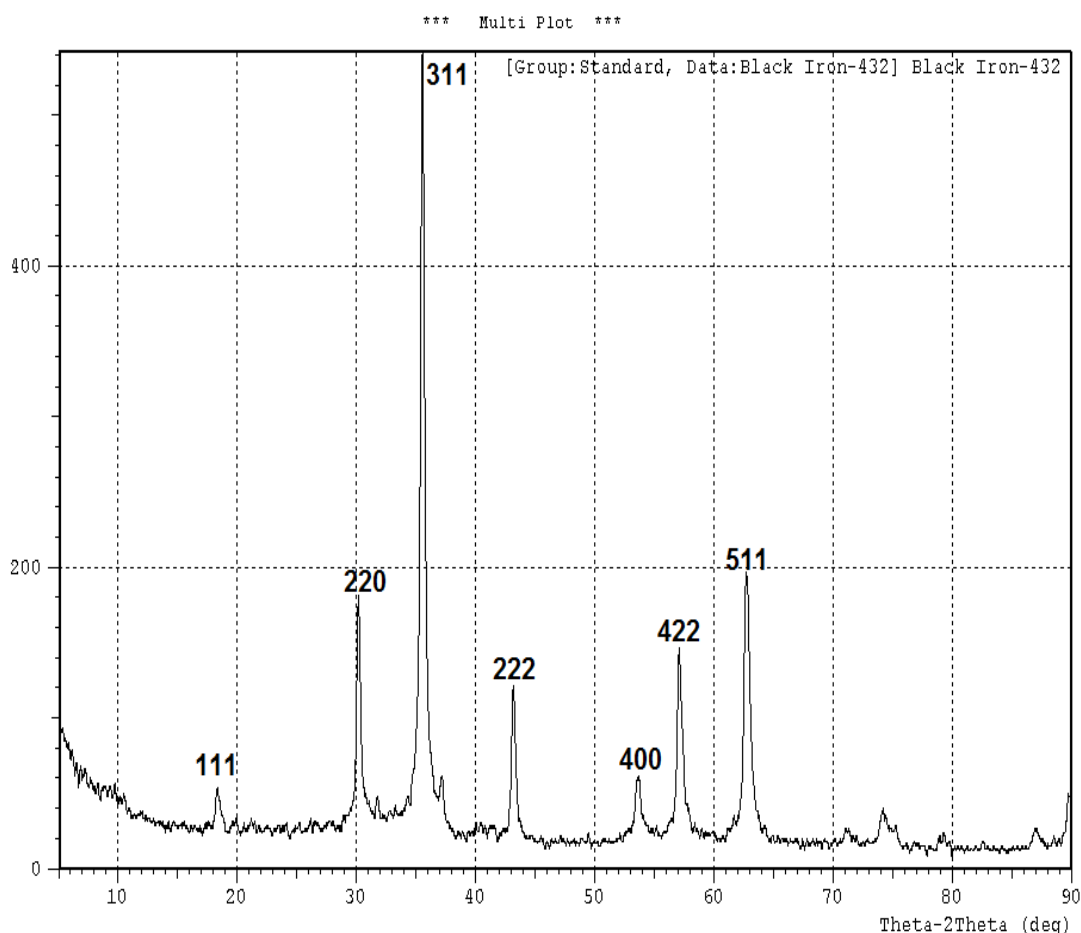


**Figure 2.** XRD of synthesized magnetite nanoparticles

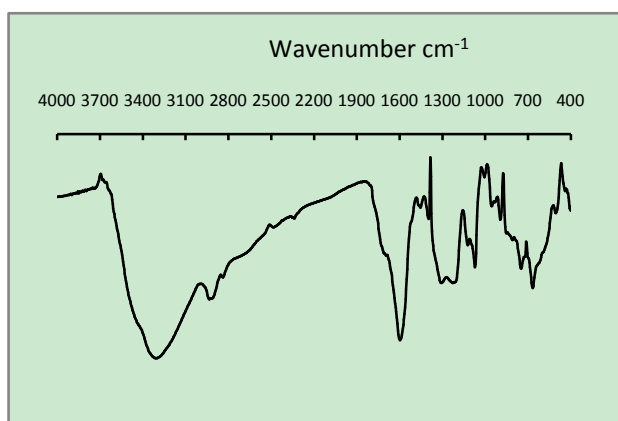


**Figure 3.** FT-IR of carob leaf extract

FT-IR spectra of synthesized magnetite nanoparticles were carried out to identify the possible biomolecules responsible for capping and stabilization of nanoparticles. Figure 4 shows the peaks associated with magnetite nanoparticles. The peaks 3410-3699, 1415 and 1029  $\text{cm}^{-1}$  have been assigned to the C-H stretching, O-H stretching, N-H stretching and bending vibration of amine  $\text{NH}_2$  group in carob leaf extract and the overlap of the stretching vibration of O-H. The peaks at 1415 and 1029  $\text{cm}^{-1}$  are attributed to the asymmetric and symmetric stretching vibration of  $\text{COO}^-$ . The presence of magnetite

nanoparticles can be seen by two strong absorption bands at around 553 and 470  $\text{cm}^{-1}$  which, corresponding to the Fe-O stretching band of bulk magnetite ( $\text{Fe}_3\text{O}_4$ ). These results revealed that the C=O groups were bonded on the magnetite particle surface. Overall the observation confirms the presence of protein in carob leaf extract, which acts as a reducing agent and stabilizer for magnetite nanoparticles.

The scanning electron microscopy (SEM) micrograph for synthesized magnetite nanoparticles is shown in Figure 5. The particles had a rather narrow size distribution, where most of the magnetite particles were within 5-8 nm. Therefore the magnetite nanoparticles were successfully synthesized by this green method using carob leaf extract as reducing agent and stabilizer for nanoparticles.

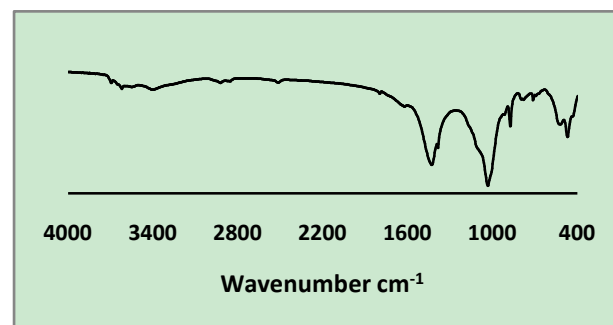


**Figure 4.** FT-IR of magnetite nanoparticles

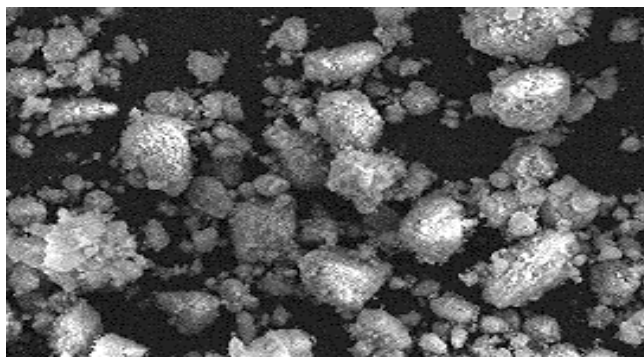


Figure 5. SEM micrograph of magnetite nanoparticles

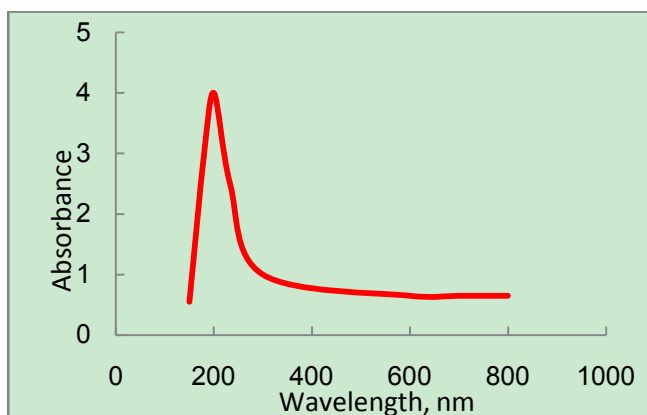


Figure 6. UV-vis absorption spectra of magnetite nanoparticles

Formation and stability of magnetite nanoparticles in aqueous colloidal solution is confirmed by using UV-vis spectral analysis. Extinction spectra of synthesized magnetite are shown in Figure 6. Characteristic surface Plasmon absorption band is observed at 233 nm for the black colour magnetite nanoparticles synthesized from ferrous chloride and ferric chloride with molar ratio 1/2 and the fixed volume 5 ml of aqueous carob leaf extract. The carob leaves extract quantities were varied from 5 to 10 ml with 100 ml of

the solution of Fe(III)/Fe(II) experimented on the synthesis of magnetite nanoparticles.

A possible formation mechanism of magnetite nanoparticles by this green method is as the following scheme, Figure 7. Ferric chloride  $\text{FeCl}_3 \cdot 6\text{H}_2\text{O}$  and ferrous chloride  $\text{FeCl}_2 \cdot 4\text{H}_2\text{O}$  and carob leaf extract are in one aqueous phase in the reaction system. The C=O of carboxylic group in carob leaf extract chelated with  $\text{Fe}^{3+}$  and  $\text{Fe}^{2+}$  to form ferric and ferrous protein. With heating,  $\text{OH}^-$  of NaOH would be involved in the reaction. A competition between of  $\text{COO}^- \text{Fe}^{3+}$  and  $\text{COO}^- \text{Fe}^{2+}$  bonds and the formation of  $\text{HO} \dots \text{Fe}^{3+}$  and  $\text{OH} \dots \text{Fe}^{2+} \dots$  bonds and a result of formation of ferric hydroxide,  $\text{Fe}(\text{OH})_3$  and ferrous hydroxide,  $\text{Fe}(\text{OH})_2$ . The formation of ferric hydroxide and ferrous hydroxide form a shell core structure with protein chain of carob leaf extract as core. Ferric hydroxide and ferrous hydroxide in core dehydrated ( $-\text{H}_2\text{O}$ ) forming magnetite ( $\text{Fe}_3\text{O}_4$ ) nanoparticle crystals. The shell of protein of carob leaf extract chains attached on  $\text{Fe}_3\text{O}_4$  surface through chelation of  $\text{COO}^- \dots \text{Fe}^{3+}$  and  $\text{COO}^- \dots \text{Fe}^{2+}$  at the end of the reaction,  $\text{Fe}_3\text{O}_4$  nanoparticle crystals were capped and stabilized by protein chain of carob leaf extract.

Thermogravimetric analysis (TGA) of magnetite nanoparticles particles is presented in Figure 8. The initial weight loss of magnetite nanoparticles powder under  $100^\circ\text{C}$  is likely to be caused by the contained water. The decomposition temperature is about  $318^\circ\text{C}$ , which is considered as the decomposition of the protein chains. From 150 to  $400^\circ\text{C}$ , decomposition of the capping agents took place. The protein of carob leaf extract decomposes completely at temperature higher than  $600^\circ\text{C}$  and the residual weight of magnetite nanoparticles is 63% at  $700^\circ\text{C}$ . The results of TGA illustrated that there is amide I and amide II in carob leaf extract in the magnetite nanoparticles with weight is around 34%. Overall the TGA demonstrated that carob leaf extract existed on the surface of magnetite nanoparticles.

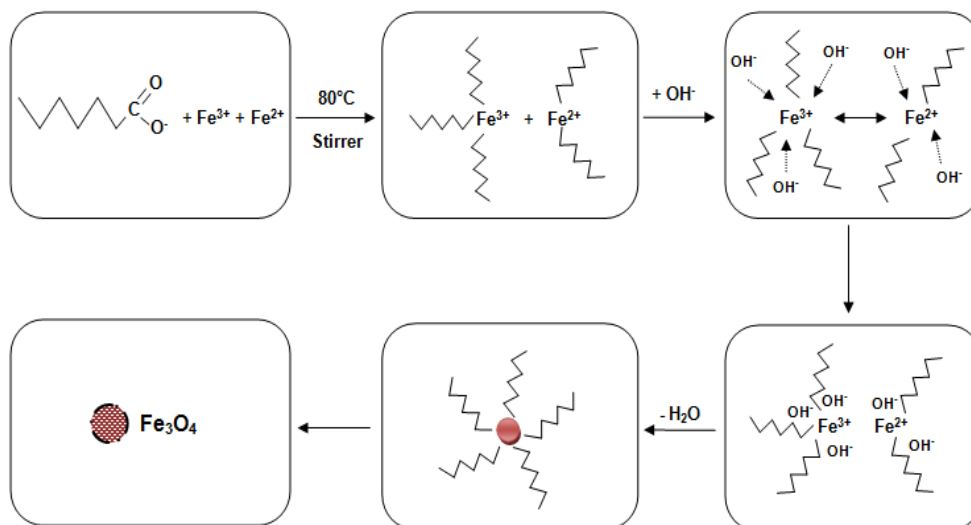


Figure 7. A schematic illustration of the formation mechanism of magnetite nanoparticles

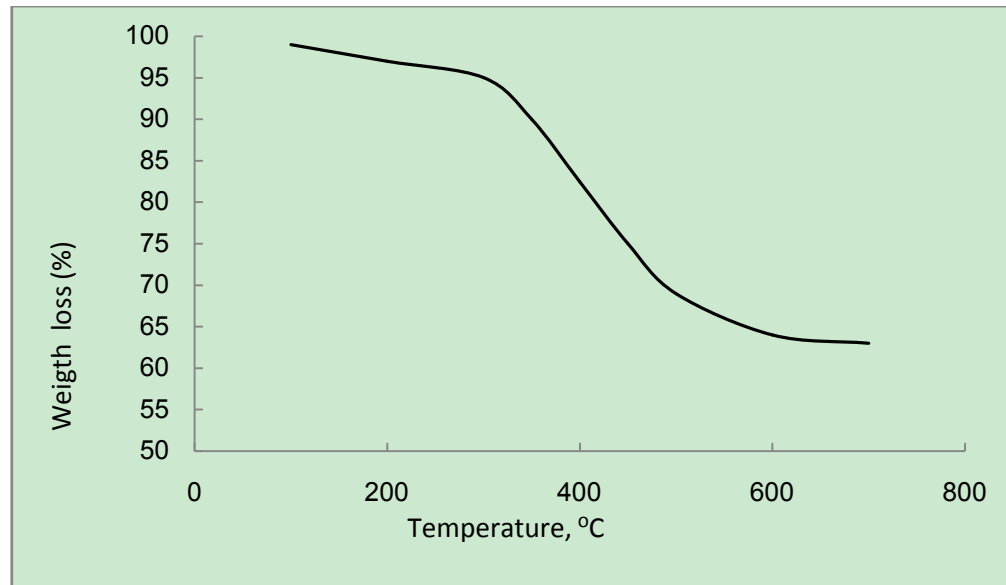


Figure 8. TGA curve of magnetite nanoparticles

## 4. Conclusions

Magnetite nanoparticles ( $\text{Fe}_3\text{O}_4$ ) were synthesized by a simple, rapid and green method in one pot reaction. The average diameter of magnetite nanoparticles is 4-8 nm and well monodisperse. The magnetite nanoparticles were capped by the carboxylic groups of amide I and amide II chains of the protein in carob leaf extract. Suspended magnetite nanoparticles obtained by this method was observed to be stable more than two weeks, indicating well-disperse in aqueous solution and prevent from aggregates. The green method in the present study has many advantageous features for synthesis magnetite nanoparticles, it is economical and environmentally friendly, non-toxic products treatment and size-controlled magnetite nanoparticles in one pot reaction at mild conditions.

## ACKNOWLEDGEMENTS

Authors gratefully acknowledge the financial support from Abdul Hameed Shoman Fund for Support Scientific Research, Amman, Jordan (Grant No. 0400. 217/28/143/18 556)

## REFERENCES

- [1] Kim J., Lee J.E., Lee J., Yu J. H., Kim B. C., An K., Hwang Y., Shin C. H., Park J. G., Kim J., Hyeon T. (2006). Magnetic Fluorescent Delivery Vehicle Using Uniform Mesoporous Silica Spheres Embedded with Monodisperse Magnetic and Semiconductor Nanocrystals. *J. Amer. Chem. Soc.*, 128: 688-689.
- [2] Kim J., Lee J.E., Lee J., Yu J. H., Kim B. C., An K., Hwang Y., Shin C. H., Park J. G., Kim J., Hyeon T. (2006). Magnetic Fluorescent Delivery Vehicle Using Uniform Mesoporous Silica Spheres Embedded with Monodisperse Magnetic and Semiconductor Nanocrystals. *J. Amer. Chem. Soc.*, 128: 688-689.
- [3] Jun Y. W., Huh Y. M., Choi J. S., Lee J. H., Song H. T., Kim S., Kim S., Yoon S., Kim K. S., Shin J. S., Suh J. S., Cheon J. (2005). Nanoscale Size Effect of Magnetic Nanocrystals and Their Utilization for Cancer Diagnosis via Magnetic Resonance Imaging. *J. Amer. Chem. Soc.*, 127: 5732-5733
- [4] Song H. T., Choi J. S., Huh Y. M., Kim S., Jun Y. W., Suh J. S., Cheon T. (2005). Surface Modulation of Magnetic Nanocrystals in the Development of Highly Efficient Magnetic Resonance Probes for Intracellular Labeling. *J. Amer. Chem. Soc.*, 127: 9992-9993.
- [5] Breteanu O., Verne E., Coisson M., Tiberto P., Allia P. (2006). Magnetic properties of the ferrimagnetic glass-ceramics for hyperthermia. *Journal of Magnetism and magnetic materials*, 305: 529-533.
- [6] Johannsen M., Gneveckow U., Taymoorian K., Thiesen B., Waldofner N., Scholz R., Jung K., Jordan A., Wust P., Loening S. A. (2007). Morbidity and quality of life during radiotherapy using magnetic nanoparticles in locally recurrent prostate cancer: Results of a prospective phase I trial. *International J. Hypertherm.*, 23: 315-323.
- [7] McCloskey K. E., Chalmers J. J., Zborowski M. (2003). Magnetic cell separation: characterization of magnetophoretic mobility. *Anal. Chem.*, 75: 6868-6874.
- [8] Gupta A. K., Wells S., (2004). Surface-modified superparamagnetic nanoparticles for drug delivery: preparation, characterization and cytotoxicity studies. *IEEE Trans. Nanobiosci.*, 3: 66-73.
- [9] Wei, X., Viadero, R.C. (2007). Synthesis of magnetite nanoparticles with ferric iron recovered from acid mine drainage: Implications for environmental engineering. *Colloids and Surfaces A: Physicochem. Aspects*, 294: 280-286.
- [10] Hu J., Lo I. M. C., Chen G., (2004). Removal of Cr(VI) by magnetite nanoparticle. *Water Sci. Technol.*, 50: 139-146.

- [11] Maity D, Chandrasekharan P, Yang CT, Chuang KH, Shuter B, Xue JM, Ding J, Feng SS (2010). Facile synthesis of water-stable magnetite nanoparticles for clinical MRI and magnetic hyperthermia applications. *Nanomedicine* 5: 1571-1584.
- [12] Yu W., Zhang T., Zhang J., Qiao X., Yang L., Liu Y. (2006). The synthesis of octahedral nanoparticles of magnetite. *Materials Letters*, 60: 2998-3001.
- [13] Zhu Y., Wu Q. (1999). Synthesis of magnetite nanoparticles by precipitation with forced mixing. *Journal of Nanoparticle Research*, 1: 393-396.
- [14] El Ghandoor H., Zidan H. M., Khalil M. M. H., Ismail M. I. M. (2012). Synthesis and some physical properties of magnetite (Fe<sub>3</sub>O<sub>4</sub>) nanoparticles. *Int. J. Electrochem. Sci.*, 7: 5734-5745.
- [15] Maity D., Kale S.N., Kaul-Ghanekar R., Xue J-M, Ding J. (2009). Studies of magnetite nanoparticles synthesized by thermal decomposition of iron (III) acetylacetonate in tri(ethylene glycol). *Journal of Magnetism and magnetic Materials*, 321:3093-3098.
- [16] Woo K., Hong j., Choi S., Lee H.W., Ahn J.P., Kim C.S., Lee S.W. (2004). Easy synthesis of magnetite properties of iron oxide nanoparticles. *Chemistry of Materials*, 16: 2814-2818.
- [17] Rockenberger J., Scher E.C., Alivisatos A.P. (1999). A New Nonhydrolytic Single-Precursor Approach to Surfactant-Capped Nanocrystals of Transition Metal Oxides. *J. Amer. Chem. Soc.*, 121: 11595-11596.
- [18] Cai W., Wan J. (2007). Facile synthesis of superparamagnetic magnetite nanoparticles in liquid polyols. *Journal of Colloid and Interface Sci.*, 305:366-370.
- [19] Xu J., Yang H., Fu W., Du K., Sui Y., Chen J., Zeng Y., Li M., Zou G. (2007). Preparation and magnetic properties of magnetite nanoparticles by sol-gel method. *Journal of Magnetism and magnetic Materials*, 309: 307-311.
- [20] Vijayakumar R., Kolytyn Y., Felner I., Gedanken A. (2000). Sonochemical synthesis and characterization of pure nanometer-sized Fe<sub>3</sub>O<sub>4</sub> particles. *Mater. Sci. Eng A:Struct. Mater. Prop. Microstructure Process*, 286: 101-105.
- [21] Dang F., Enomoto N., Hongo J., Enpuku K. (2009). Sonochemical synthesis of monodispersed magnetite nanoparticles by using an ethanol-water mixed solvent. *Ultrasonics Sonochemistry*, 16: 649-654.
- [22] Pei W., Kumada H., Saito H., Ishio S. (2007). Study on magnetite nanoparticles synthesized by chemical method. *Journal of Magnetism and Magnetic Materials*, 310: 2375-2377.
- [23] Zhang W., Shen F., Hong R. (2011). Solvothermal synthesis of magnetite Fe<sub>3</sub>O<sub>4</sub> microparticles via self-assembly of Fe<sub>3</sub>O<sub>4</sub> nanoparticles. *Particuology*, 9: 179-186.
- [24] Mizutani N., Iwasaki T., Watano S., Yanagida T., Tanaka H., Kawai, T. (2008). Effect of ferrous/ferric ions molar ratio on reaction mechanism for hydrothermal synthesis of magnetite nanoparticles. *Bull. Mater. Sci.*, 31: 713-717.
- [25] Han C, Cai W, Tang W, Wang G, Liang C (2011). Protein assisted hydrothermal synthesis of ultrafine magnetite. *Journal of 1188-11196. Materials Chemistry*, 21: 1
- [26] Bretcanu O., Verné E., Coisson M., Tiberto P., Allia P. (2006). Magnetic properties of the ferrimagnetic glass-ceramics for hyperthermia. *Journal of Magnetism and Magnetic Materials*, 305: 529-533.
- [27] Jun Y.W., Huh Y.M., Choi J.S., Lee J.H., Song H.T., Sungjun H.T., Yoon S., Kim K.S., Shin J.S., Suh J.S., Cheon J. (2005). Nanoscale size effect of magnetic nanocrystals and their utilization for cancer diagnosis resonance. *Journal of American Chem. Soc.*, 127: 5732-5733.
- [28] Song H.T., Choi J.S., Huh Y.M., Kim S., Jun Y.W., Suh J.S., Suh J. (2005). Surface modulation of magnetic nanocrystals in the development of highly efficient magnetic resonance probes for intracellular labeling. *Journal of Amer. Chem. Soc.*, 127: 9992-9993.
- [29] Klug H.P., Alexander L.E. X-ray diffraction procedures for polycrystalline and amorphous materials, Wiley, New York (1954).